Catalysis of the Decomposition of Hydrogen Peroxide by a Complex of Iron(III) with a Synthetic Macrocyclic Ligand

Alexandra C. Melnyk, Nicholas K. Kildahl, Alan R. Rendina, and Daryle H. Busch*

Contribution from The Evans Chemical Laboratory, The Ohio State University, Columbus, Ohio 43210. *Received April 13, 1978*

Abstract: The complex dichloro-*meso*-2,12-dimethyl-3,7,11,17-tetraazabicyclo[11.3.1]heptadeca-1(17),13,15-trieneiron(III) tetrafluoroborate, abbreviated $[Fe(CRH_4)Cl_2]BF_4$, is an effective catalyst for the decomposition of H_2O_2 to form H_2O and O_2 in aqueous solution. The solution behavior of the complex $[Fe(CRH_4)Cl_2]BF_4$ was studied in order to facilitate the analysis of the rate data. The iron complex exists primarily as the aquo-hydroxo complex in the pH range of interest. This aquo-hydroxo complex slowly self-condenses in the presence of air and acetate buffers to give an antiferromagnetically coupled, μ-oxo dimer. The dimerization rate has been measured. The active species in the catalysis of H_2O_2 decomposition is the aquo-hydroxo complex $Fe(CRH_4)(OH)(H_2O)^{2+}$. The dimer is catalytically inactive, as is the corresponding dimer of hemin. The kinetics of H_2O_2 decomposition in the pH range from 3.8 to 5.1 and in the temperature range from 8 to 32 °C were studied thoroughly by oxygen evolution measurements using an apparatus which allows very rapid pressure changes to be monitored. The observed rate law is shown to be consistent with a mechanism formulated in terms of free-radical intermediates. Acetate inhibits the reaction, possibly by competing for hydroxyl radicals.

Introduction

Since the early 19th century the catalytic decomposition of H_2O_2 has been viewed with extreme interest. The action of the enzyme which is responsible for accelerating this decomposition in living organisms was first observed indirectly in 1811 by Thenard,[1] who noted that the tissue of plants and animals was able to decompose hydrogen peroxide to water and oxygen. It was not until 1911, however, that the enzyme catalase was identified and isolated by Wolff and Stoecklin.[2] Since that time, the nature and catalytic activity of catalase have been the subjects of extensive research.

Catalase is a heme iron protein having a molecular weight of about 250 000 and containing four hemin groups per molecule, each hemin moiety consisting of high-spin iron(III) in a protoporphyrin IX ring. It is usually assumed that the fifth and sixth coordination sites of iron are occupied by the imidazole ring of a histidine residue and either by a water molecule or a hydroxyl group.[3] However, the tertiary structure of the protein in catalase is as yet unknown.

The kinetics and mechanism of peroxide decomposition in the presence of catalase have been studied extensively. The reaction involves the formation of a much-studied intermediate termed compound I,[3-5] which is presently viewed as involving a 2-equiv oxidation of each catalase prosthetic group, producing Fe(IV) and a radical form of the protoporphyrin IX macrocycle. It is now fairly certain that the intermediate does *not* consist of a complex between molecular hydrogen peroxide and catalase, as suggested by Jones and Suggett,[7] since it has been found possible to generate compound I from catalase using a variety of oxidizing agents. Although formation of compound I is undoubtedly preceded by coordinate interaction between Fe(III) and H_2O_2, this is not kinetically observable.

The enzyme peroxidase, which utilizes H_2O_2 in the oxidation of certain organic substrates, also reacts via an intermediate having properties like compound I. The similarity between catalase and peroxidase compounds I led to the advancement of the peroxidatic mechanism of catalase and peroxidase action,[8-11] which is now widely accepted. This mechanism will be discussed in more detail later.

A number of model systems have been investigated which yield rate laws similar to that observed for the catalase-H_2O_2 reaction, but none of these yields an acceleration approaching that of catalase over a comparable range of pH. The simplest conceivable models, aquated ferrous and ferric ions, were investigated by Haber and Weiss,[12,14] by Baxendale, Barb, George, and Hargrave,[14] and more recently by Walling and his co-workers.[15] Work on these systems has been reviewed by Jones,[16] Martell,[17] and Walling.[15] Although both ions serve as effective catalysts at pH <2, apparently functioning via a free-radical mechanism, their tendencies to hydrolyze prevent studies in the range of pH over which catalase performs effectively.

Systems involving Fe(III) bound by various ligands have also been studied. The most obvious model of this type is the catalase prosthetic group (iron(III) protoporphyrin IX), which, when stripped of protein, maintains its ability to decompose hydrogen peroxide.[10,16,18-20] Two factors affect the kinetics of the decomposition by hemin which are not important for catalase. These are pH and the marked tendency for hemin to form oxo-bridged dimers, especially at higher pH. When these two factors are taken into account,[18-20] it is found that hemin is nearly as effective as catalase in promoting peroxide decomposition.[18] In fact, the same may be said of the hydrated ferric ion, for extrapolation of its catalytic activity to the physiological pH range gives activity comparable to that of hemin. These results suggest that two important functions of the protein portion of catalase may be to prevent dimerization and to act as an internal buffer for the heme center.

Catalysis by iron(III) phthalocyanine has been examined and is probably heterogeneous owing to the low solubility of the complex in water.[21] The best synthetic catalyst reported to date is the iron(III) complex of triethylenetetramine (trien), investigated by Wang.[22-25] This species performs its most effective catalysis near pH 10, where the second-order rate constant for peroxide decomposition is 1.2×10^3 M^{-1} s^{-1}. The Fe(III) complex of tris-2-aminoethylamine (TAEA) was also investigated and found to exhibit a similar catalytic behavior. Subsequent work by Beck and Gorog[26,27] on these systems revealed that, under the pH conditions used, the amine ligands were decomposed and the ferric ion hydrolyzed, but that the kinetic results obtained by Wang were reproducible. So, although the exact nature of the catalytically active species is unknown, catalysis is quite effective at pH values where catalase itself functions effectively.

A related model which is also effective in the pH range 9-10 is the Fe^{III}-EDTA complex investigated by Walling, Kurz, and Schugar.[28] Although their kinetic studies were somewhat limited, their results indicate a first-order dependence on the iron concentration and a zero-order dependence on peroxide concentration over most of the range of reaction conditions.

0002-7863/79/1501-3232$01.00/0

At lower pH they found that peroxide destroys EDTA, producing CO_2 and ammonia. In addition, the complex shows peroxidatic activity toward several substrates in the presence of hydrogen peroxide. These workers also investigated cyclohexenediaminetetraacetic acid, *N*-hydroxyethylethylenediamine triacetate, and nitrilotriacetic acid as ferric ion chelating agents. The resulting complexes were found to catalyze peroxide decomposition in similar pH ranges and with rates similar to those of the EDTA complex, but with complicated kinetic behavior.

Our interest in synthetic macrocyclic ligands and their complexes with transition-metal ions has led us to investigate the possibility that iron(III) complexes of such ligands[29] might serve as effective catalysts for the decomposition of H_2O_2. Dichloro-*meso*-2,12-dimethyl-3,7,11,17-tetraazabicyclo-[11.3.1]heptadeca-1(17),13,15-trieneiron(III) tetrafluoroborate, abbreviated $[Fe(CRH_4)Cl_2]BF_4$ (structure I), has been

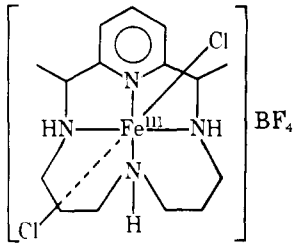

I

found to catalyze the decomposition of H_2O_2 in aqueous solution. It is readily soluble in water and its dilute aqueous solutions remain clear on standing for hours, indicating that hydrolysis is slow. We report here detailed kinetic studies of peroxide decomposition in the presence of $[Fe(CRH_4)Cl_2]BF_4$, supplemented by observations on the hydrolytic behavior of the complex over time periods applicable to the kinetic measurements. This represents the first report of catalysis by a synthetic macrocyclic iron(III) complex and lends support to the view that synthetic macrocycles can act as effective substitutes for the naturally occurring porphyrins in providing activating environments at transition-metal ions.

Experimental Section

Reagents for Peroxide Decomposition Kinetics. H_2O_2 (30%) was obtained from J. T. Baker Chemical Co. and used as purchased. Stock solutions 0.1–0.5 M in H_2O_2, 0.05 M in sodium acetate–acetic acid buffer (pH 4.61), and 0.45 M in KNO_3 were prepared by appropriate dilutions of 30% H_2O_2, 0.5 M acetate buffer, and 1 M KNO_3 with doubly distilled deionized water. These solutions were used for determining the rate dependences on the concentrations of H_2O_2 and $[Fe(CRH_4)Cl_2]BF_4$. Solutions for studying pH dependence in the range from 3.8 to 5.1 were prepared by varying the quantity of acetic acid used in the preparation, while maintaining the concentrations of sodium acetate and KNO_3 at 0.05 and 0.45 M, respectively. Solutions for studying acetate dependence in the concentration range from 0.01 to 0.2 M were prepared by varying the amounts of 0.5 M acetate buffer and 1 M KNO_3 used in the preparation so as to maintain the ionic strength at 0.5 M. All H_2O_2 solutions were standardized by titration against 0.1 M Ce(IV), stabilized with 1 M H_2SO_4, using either ferroin (Fisher Scientific Co.) or the first faint yellow of excess Ce(IV) as the indicator. Reproducible, precise end points were obtained by either method. The Ce(IV) solution was standardized against $K_4Fe(CN)_6$, which was used as a primary standard. Ferroin was also used as the indicator in these titrations.

Syntheses. *meso*-$CRH_4 \cdot H_2O$. The ligand *meso*-$CRH_4 \cdot H_2O$ was prepared by removal from $Ni(CRH_4)(ClO_4)_2$ following a modification of the method of Karn and Busch.[30] $Ni(CR)(ClO_4)_2$ was prepared by a previously described method,[31] and hydrogenated under 2000 lb/in.^{2} of hydrogen gas in a hydrogenation bomb.[30] The resulting $Ni(CRH_4)(ClO_4)_2$ was isolated as orange-red crystals and the ligand was removed as follows. Thirty grams (0.0577 mol) of $Ni(CRH_4)(ClO_4)_2$ was dissolved in 800 mL of hot water. To this, 22.5 g (0.346 mol) of KCN was added, causing the color of the solution to change rapidly from orange-red through violet to yellow. The resulting solution was made strongly alkaline by the addition of 1 lb of NaOH pellets. The free ligand, *meso*-$CRH_4 \cdot H_2O$, rose to the surface of the solution as a yellow oil which solidified upon cooling of the solution in a refrigerator for 12 h. The solid ligand was skimmed from the top of the solution and dissolved in hot diethyl ether. The ether solution was treated with activated charcoal, filtered through Celite and taken to dryness on a rotary evaporator. The resulting white ligand, $CRH_4 \cdot H_2O$, was collected and weighed, yield 90%. Anal. Calcd for $C_{15}H_{23}N_4O$: C, 64.25; H, 10.07; N, 19.98. Found: C, 64.16; H, 10.21; N, 19.87.

$Fe(CRH_4)Cl_2$. The complex was prepared by the method of Merrell and Busch.[29]

$[Fe(CRH_4)Cl_2]BF_4$. In a typical preparation, 1.0 g (2.57 mmol) of $Fe(CRH_4)Cl_2$ was dissolved in about 30 mL of 1:1 ethanol–CH_3CN (v/v) under an inert atmosphere to yield a yellow solution. To the yellow solution, 1 mL of 48% HBF_4 was added and air was bubbled through the solution for approximately 0.5 h to yield a gold solution. The volume was reduced on a rotary evaporator until gold crystals began to separate. An additional 10 mL of ethanol was added and the volume was further reduced to about 15 mL. The gold crystals of the product were separated by filtration, washed with ether, and recrystallized once from CH_3CN–ethanol. The reprecipitated crystals were washed with ether, dried in vacuo, and characterized by elemental analyses and IR. Anal. Calcd for $FeC_{15}H_{26}N_4Cl_2BF_4$: C, 37.85; H, 5.51; N, 11.77. Found: C, 37.63; H, 5.79; N, 11.22.

Solvents. Reagent grade acetonitrile and ethanol were used in the synthesis of $[Fe(CRH_4)Cl_2]BF_4$. Both solvents were dried and deoxygenated by refluxing over CaH_2 under N_2 for 12 h, followed by distillation from CaH_2 under N_2.

Doubly distilled deionized water was used in the hydrolytic and rate studies.

Physicsl Measurements. Hydrolytic Behavior of $[Fe(CRH_4)Cl_2]BF_4$. Conductance Measurements. The conductances of aqueous solutions of $[Fe(CRH_4)Cl_2]BF_4$ were measured with an Industrial Instruments Model RC16B_2 conductivity bridge using a conductivity cell with cell constant of 2.120 cm^{-1}. Conductivity-grade water was used for these measurements.

Potentiometric Titrations. Potentiometric titrations of aqueous solutions of $[Fe(CRH_4)Cl_2]BF_4$ were monitored with an expanding-scale Corning pH meter, Model 12, equipped with a Corning glass electrode and a saturated calomel reference electrode. Prior to each titration, the pH meter was calibrated with four buffer solutions (pH 3, 5, 7.2, and 8) obtained from Fisher Scientific Co.

Solutions of $[Fe(CRH_4)Cl_2]BF_4$ for potentiometric measurements were prepared using doubly distilled, deionized water. For the titrations performed under nitrogen, the water was refluxed for 0.5 h under N_2 to remove dissolved oxygen before use. Solutions were prepared under N_2 and a continuous purge of N_2 through the solution was maintained during the titration. Concentrations of $[Fe(CRH_4)Cl_2]BF_4$ in the range 0.001–0.01 M were used and the ionic strength was maintained at 0.1 M using KNO_3. Standardized solutions of NaOH in the concentration range between 0.06 and 1.2 N were used as titrant. All NaOH solutions were standardized against potassium acid phthalate using phenolphthalein as indicator.

Electronic Spectra. Electronic spectra of 0.000 22–0.02 M solutions of $[Fe(CRH_4)Cl_2]BF_4$ in water or acetic acid buffer were measured using 5-cm, 1-cm, and 1-mm matched quartz cells equipped with ground glass or Teflon stoppers. A Cary Model 14R spectrophotometer equipped with a high-intensity light source was used for the recording of spectra in the range from 1200 to 220 nm.

The kinetics of formation of the bridged dimeric species of Fe(III) were monitored at 492 nm using a Cary Model 1605 spectrophotometer equipped with a carousel cell holder and a Cary Model 1629 programmer which rotates the holder at definite time intervals. Each cell has automatic regulation of the absorbance range, controlled by a Cary Model 1627 multizero suppression attachment. Solutions for the kinetic studies were prepared in situ in the quartz cells and the absorbance was monitored as a function of time.

Infrared Spectra. IR spectra of solids were obtained on KBr pellets using a Perkin-Elmer 337 grating spectrophotometer. Spectra of aqueous solutions of $[Fe(CRH_4)Cl_2]BF_4$ were measured on Perkin-Elmer Model 337 and 457 spectrophotometers using disposable matched AgCl cells supplied by Research and Industrial Instrument Co., London.

pH Measurements. pH measurements were made using either a Corning Model 12 pH meter with expanded scale or a Beckman Model G pH meter. Corning glass electrodes and saturated calomel reference electrodes were used with both types of meter.

Solution Magnetic Susceptibility Studies. Solution magnetic susceptibilities were measured by the Evans method[32] on aqueous solutions of $[Fe(CRH_4)Cl_2]BF_4$ both in the presence and absence of acetate buffer with a Varian A-60A spectrometer operating at a probe temperature of 38–40 °C. Diamagnetic corrections were made using an experimentally determined value for the macrocyclic ligand, CRH_4,[33] and Pascal's constants for Cl^- and BF_4^-.

Calculation of pK_a Values. Data from the potentiometric titrations were subjected to computer analysis using the program SCOGS (stability constants of generalized species) and an associated subroutine COGSNR (concentrations of generalized species by the Newton–Raphson method) developed by I. G. Sayce.[34]

Kinetics of Peroxide Decomposition by O_2 Evolution. The kinetics of peroxide decomposition were studied by measuring the rate of O_2 evolution into a vacuum system of known constant volume. The pressure in the system was monitored with a Texas Instruments precision pressure gage, Model 145, equipped with a type 1 Bourdon tube capsule designed for the measurement of differential pressures at line pressures of up to 3000 Torr. The Bourdon tube was thermostated at a temperature of 44 °C. The precision pressure gage was used in conjunction with a Hewlett-Packard Model 7101 BM recorder to produce a direct trace of the pressure-time profile. Commercial specifications state the full scale response time of the recorder to be 0.5 s. It was observed that the actual response time is about 0.1 s, or about 1 atm/s for a typical recorder sensitivity setting, far exceeding the specifications.

Decomposition of hydrogen peroxide was initiated by shaking a reaction vessel (vide infra) containing initially separated peroxide and catalyst solutions. Shaking was effected by a Burrell wrist action shaker which was modified to provide greater shaking amplitude than was characteristic of the commercial apparatus.

Two types of reaction vessels were used. Type 1 consisted of a 125-mL Erlenmeyer flask equipped with a 6-in. neck and a ground glass joint. The flask could be attached to the vacuum manifold via a piece of Tygon tubing. Type 2 consisted of a thick-walled 250-mL suction flask, which could be connected to the vacuum manifold by a piece of Tygon tubing attached to the side arm of the flask and sealed with a tight-fitting rubber stopper. The two types of reaction vessel gave the same results, but the suction flasks better withstood the violent action of the shaker.

H_2O_2 solution (25 mL) was pipetted into the reaction flask and the flask was allowed to equilibrate in a constant-temperature water bath for 10 min. $[Fe(CRH_4)Cl_2]BF_4$ solution (2 mL) was pipetted into a small glass vial approximately 1.5 cm in diameter and 3 cm deep. This vial, which contained a 1-in. Teflon-coated magnetic stirring bar, was then lowered into the Erlenmeyer flask containing the peroxide solution. The flask was mounted in the shaker and connected to the vacuum line, which contained air at atmospheric pressure saturated with water vapor, and the vacuum line was closed to the atmosphere. Reaction was initiated by activating the shaker. The rapid evolution of O_2 which resulted from mixing of the solutions was manifested as a trace on the recorder. The initial slope of the trace gave the initial rate of O_2 evolution in mol/s, after the proper units conversions[35] were made. Immediately following reaction, the contents of the reaction flask was titrated for H_2O_2 using Ce^{4+}. The moles of peroxide remaining were compared with the moles of O_2 produced (as calculated from the recorder deflection) and were found to satisfy the stoichiometry implied by the equation

$$2H_2O_2 \rightarrow 2H_2O + O_2$$

In all cases, the peroxide solutions were buffered with 0.05 M sodium acetate–acetic acid. Ionic strengths of both catalyst and peroxide solutions were maintained at 0.5 M using KNO_3. All reported rates represent averages of at least three and sometimes as many as 12 individual runs, with an average deviation of 10%. Occasional blank runs were performed to determine whether significant peroxide decomposition occurred in the absence of catalyst. O_2 evolution was observed *only* in the presence of $[Fe(CRH_4)Cl_2]BF_4$.

Results

Species Present in Unhydrolyzed Solutions of $[Fe(CRH_4)Cl_2)]BF_4$. Solutions of the catalyst $[Fe(CRH_4)Cl_2]BF_4$ clearly contain different species depending on their histories. In order to be able to analyze the results of kinetic studies intelligently it is necessary to understand the solution behavior of the resting catalyst.

The lability of complexes of high-spin iron(III) leads one to anticipate the replacement of both chlorides from $Fe(CRH_4)Cl_2^+$ by water molecules. The molar conductances of 9.07×10^{-4} and 8.655×10^{-4} M aqueous solutions of $[Fe(CRH_4)Cl_2]BF_4$ were found to be 584 and 533 Ω^{-1} cm^{-1}, respectively. The molar conductances are consistent with the assumption that both chlorides are dissociated yielding the ion $Fe(CRH_4)(H_2O)_2^{3+}$ which may be partially ionized as shown in the equation

$$Fe(CRH_4)(H_2O)_2^{3+} \rightarrow Fe(CRH_4)(H_2O)(OH)^{2+} + H^+ \quad (1)$$

The diaquo complex has been characterized by means of potentiometric titrations. The measurements apropos of this species were carried out as quickly as possible (fast titrations) and the pH values used were those observed immediately after the addition of NaOH to the solution. (It will be shown below that different results occur if the titration is performed slowly enough to include a slow hydrolysis process.) The titration curves show two equivalence points at ratios of moles NaOH added to moles of $[Fe(CRH_4)Cl_2]BF_4$ of 1 and 2. The fast titration curves for solutions containing 0.001, 0.002, 0.003, 0.004, 0.006, and 0.008 M $[Fe(CRH_4)Cl_2]BF_4$ are superimposable up to pH 8. Above pH 8 the curves change with concentration if the titration is carried out in the presence of air. This suggests polymerization and is discussed in the next section.

The superimposability of the titration curves below pH 8 suggests the absence of polynuclear species under these conditions. Assuming that only reactions 1 and 2 contribute to the behavior observed during the fast titrations,

$$[Fe(CRH_4)(H_2O)(OH)]^{2+} \rightarrow [Fe(CRH_4)(OH)_2]^+ + H^+ \quad (2)$$

the calculated values of pK_{a_1} and pK_{a_2} were 2.88 ± 0.02 and 7.43 ± 0.03, respectively, with a standard deviation in titer of 0.24 mL per 100 mL of solution. This small standard deviation indicates that the assumed acid-dissociation reactions are most likely the only pH-dependent reactions occurring to a significant extent below pH 8.3 in the solutions being titrated.

The electronic spectrum of aqueous $[Fe(CRH_4)Cl_2]BF_4$ shows two strong bands in the ultraviolet (λ_{max} 252 nm (ϵ 8740), λ_{max} 205 (14 000) and a weak band in the visible region, at 520 nm (ϵ 8.33). These are considered to be characteristic of $Fe(CRH_4)(H_2O)_2^{3+}$. At high dilution it was possible to observe a weak shoulder at 272 nm which is not evident in more concentrated solutions. The fact that this shoulder appears only at high dilution suggests that it is attributable to the acid dissociation product of the aquated complex, i.e., the monohydroxo complex formed in accord with eq 1. The absorbance at 272 nm varies linearly with the concentration of $[Fe(CRH_4)(H_2O)(OH)]^{2+}$ as calculated from pK_{a_1} thereby confirming the assignment.

The kinetic studies reported here for the catalyst $[Fe(CRH_4)Cl_2]BF_4$ made use of acetate buffers. It was therefore necessary to determine the extent of complexation between the acetate ion and the ions derived from the catalyst. This was accomplished by performing titrations on solutions prepared from the iron complex and acetic acid. The molar ratio of $[Fe(CRH_4)Cl_2]BF_4$ to $HC_2H_3O_2$ was maintained at either 1:1 or 1:5 during these experiments. Only fast titrations were performed. Curves resulting from the titration performed in air exhibit three equivalence points at $N = 1$, 2, and 3 and three buffer regions. Above pH 5, the third buffer region shifts

toward higher pH with higher concentration of iron complex, similar to the behavior that was observed for titrations performed in the absence of acetic acid. Using the pK_{a_1} and the pK_{a_2} values obtained from the previous potentiometric titrations and the pK_a values for acetic acid as initial input to the SCOGS program, the first two buffer regions were submitted to computer analysis. The calculated pK values of 2.835 ± 0.014 and 4.812 ± 0.017 are consistent with reactions 1 and 3

$$HC_2H_3O_2 = H^+ + C_2H_3O_2^- \quad (3)$$

being the only pH-dependent processes occurring to a significant extent below pH 5.1. The small standard deviation in titer of 0.0135 mL per 50 mL initial volume of solution supports this conclusion. If significant interaction were occurring between $Fe(CRH_4)(H_2O)(OH)^{2+}$ and acetate ion, deviations from the normal pK for acetic acid should be observed.

The studies on peroxide decomposition that constitute the main body of this report were conducted over the pH range from 3.94 to 5.10. Under those pH conditions, using acetate buffer, and with stock solutions prepared as described here, the only important iron-containing species are those appearing in eq 1 and 2. $Fe(CRH_4)(OH)(H_2O)^{2+}$ is the predominant species in the pH range used. As the following section shows, dimeric complexes form in stock solutions prepared under certain specific conditions.

Dimer Formation in Solutions of $[Fe(CRH_4)Cl_2]BF_4$. Initial studies on the catalytic decomposition of hydrogen peroxide using $[Fe(CRH_4)Cl_2]BF_4$ showed a complicated dependence of rate on catalyst concentration. This has been traced to the formation of dimeric complexes in certain stock solutions. The dimers were shown to be catalytically inactive. Dimerization occurs in stock solutions prepared by dissolving the iron complex in acetate buffer solution in the presence of air.

Potentiometric titrations that are performed very slowly (allow time for complete equilibration after each addition of NaOH) show evidence of some kind of polymerization process. Such a titration requires 4–6 h. Curves resulting from the titration of dilute solutions of $[Fe(CRH_4)Cl_2]BF_4$ (<0.002 M) again show two equivalence points, at $N = 1$ and 2, but the position of the second buffer region is strongly concentration dependent. This behavior indicates that hydrolysis is occurring at higher pH on a slow time scale. The slow titration curves of 0.003 and 0.004 M solutions, on the other hand, show equivalence points at $N = 0.5$, 1, and 1.5. Similar behavior was exhibited by a 0.004 M solution which had been aged for 14 h. These results provide strong support for significant dimerization of the complex in more concentrated solutions. An aged 0.001 M solution showed equivalence points only at $N = 1$ and 2, indicating that dimerization occurs only in more concentrated solutions.

The magnetic susceptibilities of aqueous solutions of $[Fe(CRH_4)Cl_2]BF_4$ in the absence and presence of acetate buffer provide evidence for an antiferromagnetic dimer. A 0.012 M solution of $[Fe(CRH_4)Cl_2]BF_4$ in water gave a magnetic moment per iron of 5.75 μ_B, quite close to the value of 5.92 μ_B expected for the spin-only moment of high-spin Fe(III). On the other hand, a 0.012 M solution of $[Fe(CRH_4)Cl_2]BF_4$ in water containing 0.3 M acetate buffer gave a magnetic moment of only 4.37 μ_B per iron atom, far below that expected for high-spin iron(III).

Conclusive proof that $[Fe(CRH_4)Cl_2]BF_4$ forms an antiferromagnetically coupled dimer came from electronic spectral studies. It has long been known that the electronic spectra of dimeric iron(III) complexes show a number of simultaneous transitions at frequencies that are algebraic sums of the frequencies of the separate (spin-forbidden) transitions.[36] This behavior is so distinctive that its observation requires the presence of dimeric species. Solutions of $[Fe(CRH_4)Cl_2]BF_4$ in air-saturated acetate buffers show such a series of relatively sharp absorption maxima throughout the visible and near-ultraviolet ranges of their electronic spectra. The maxima appear immediately upon dissolution of the complex and their intensities increase with time. The kinetics of these processes are described below.

Table I. Electronic Spectral Data for Oxo-Bridged Fe(III) Dimers

assignment	obsd energy, cm^{-1}	calcd energy, cm^{-1}
	$[Fe(CRH_4)(H_2O)]_2O^{4+}$ [a]	
a. $^6A_1 \rightarrow {}^4T_1(^4G)$	8 928	8 897
b $^6A_1 \rightarrow {}^4T_2(^4G)$	14 992	14 945
	19 685	
c. $^6A_1 \rightarrow {}^4A_1, {}^4E(^4G)$	20 280	20 285
d $^6A_1 \rightarrow {}^4T_2(^4D)$	22 026	22 814
a + b	23 753	23 920
a + c	29 411	29 208
b + c	35 088	35 272
b + d	37 500	37 018
c + d	42 553	42 306
	$[FeEDTA]_2O^{4-}$ [b]	
a. $^6A_1 \rightarrow {}^4T_1(^4G)$	11 300	
b. $^6A_1 \rightarrow {}^4T_2(^4G)$	18 400	
c. $^6A_1 \rightarrow ({}^4A_1, {}^4E)({}^4G)$	21 000	
d. $^6A_1 \rightarrow {}^4T_2(^4D)$	24 700	
a + b	29 100	29 700
a + c	32 400	32 300
b + b	36 800	36 800
b + c	40 700	39 400
	Diaquo Methemerythrin[c]	
a. $^6A_1 \rightarrow {}^4T_1(^4G)$	9 000[d]	
b. $^6A_1 \rightarrow {}^4T_2(^4G)$	14 706	
c. $^6A_1 \rightarrow ({}^4A_1, {}^4E)({}^4G)$	20 367	
d. $^6A_1 \rightarrow {}^4T_2(^4D)$	22 222	
a + b	23 256	23 706
a + b	24 096	23 706
	27 248	
b + b	29 851	29 472
a + c		29 367
a + d	31 847	31 150
a + f	33 557	33 096

[a] This work. [b] Reference 39. [c] Reference 36. [d] The 9000-cm^{-1} band is assumed.

The absorption maxima, their assignments, and calculated values for the combination bands are given in Table I. Other examples are included for comparison. The agreement is unequivocal. Note that the low-energy bands are assigned to single d–d transitions; they fit the ligand field model with Dq = 1225 cm^{-1}, B = 843 cm^{-1}, and C = 2371 cm^{-1}. The remaining five transitions are assigned to simultaneous two-electron excitations and, as stated earlier, the agreement is excellent.

The electronic spectrum given in Table I was observed *only* in solutions prepared in air-saturated buffers. Such solutions showed a characteristic green color. Solutions prepared in degassed acetate buffer are yellow and their solutions do not exhibit the abundance of electronic spectral bands. When air was subsequently introduced to these solutions, neither the color nor the electronic spectra were altered. It must be concluded that both air and acetate are required to produce this spectrum, and in that order. This behavior may imply oxidative dehydrogenation of the macrocyclic ligand prior to dimer formation. There is precedent for oxidative dehydrogenation of macrocyclic ligands coordinated to both Fe(II)[37] and Fe(III)[38] but the suggestion of such a process for the present systems is speculative.

An absorption band at 33 900 cm^{-1}, not included in Table I, appears only in dilute systems (<10^{-4} M). It is assigned to

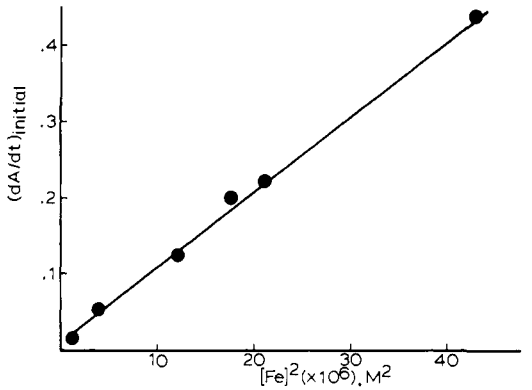

Figure 1. Dimerization rate. Variation of initial rate of change of absorbance (dA/dt) with the square of the concentration of $[Fe(CRH_4)Cl_2]BF_4$.

the presence of monomeric complexes. Dilution of solutions of the dimer does not produce this band. This suggests that the dimer is either stable or very slow to dissociate.

The rate of dimer formation was measured spectrophotometrically at 492 nm using acetate buffer solutions (0.05 M in buffer, pH 4.6) of $[Fe(CRH_4)Cl_2]BF_4$. Initial rates were determined by measuring dA/dt at $t = 0$ using the mirror technique. A plot of dA/dt vs. the square of the concentration of $[Fe(CRH_4)Cl_2]BF_4$ (Figure 1) is linear with a slope equal to the second-order dimer formation rate constant. The value of the observed rate constant at 25 °C is 0.982×10^4 min^{-1} M^{-2}, as determined from the least-squares slope of the graph.

The studies summarized to here provide the understanding of the solution behavior that is necessary in order to analyze the results of studies on the kinetics of decomposition of H_2O_2 under the influence of $[Fe(CRH_4)Cl_2]BF_4$. The critical relationships are as follows.

1. Stock solutions of $[Fe(CRH_4)Cl_4]BF_4$ contain the ions $Fe(CRH_4)(H_2O)_2^{3+}$, $Fe(CRH)(OH)(H_2O)^{2+}$, and $Fe(CRH_4)(OH)_2^{+}$.

2. The relative abundances of the aquo and hydroxo ions depend on the pH ($pK_{a_1} = 2.88 \pm 0.02$ and $pK_{a_2} = 7.43 \pm 0.03$).

3. In the pH range used in the peroxide studies $Fe(CRH_4)(OH)(H_2O)^{2+}$ is the dominant species.

4. The ions derived from $[Fe(CRH_4)Cl_2]BF_4$ do not form detectable amounts of acetate complexes under the conditions used in the peroxide studies.

5. If the catalyst is dissolved in buffer solution in the presence of air, the resulting stock solution will contain the catalytically inactive dimer. This should be avoided.

Kinetics of Hydrogen Peroxide Decomposition. All of the rates are initial rates obtained by measuring the maximum slope of the experimental recorder trace representing the change of pressure of O_2 as a function of time. Therefore, the rate laws are initial rate laws, and all concentration dependences are expressed in terms of *initial* concentrations.

Dependence of Initial Rates on $[Fe(CRH_4)Cl_2]BF_4$. Both unbuffered and buffered catalyst stock solutions were used in studies of the dependence of initial rate on catalyst concentration. As will be seen below, data obtained using unbuffered catalyst stock solutions yield a linear plot of observed initial rate vs. catalyst concentration. Data obtained using buffered catalysts stock solutions, however, invariably gave curved plots. We have expended much effort to show that these curved graphs can be brought into coincidence with the linear ones by making suitable corrections for the dimerization process which is known to occur in solutions of $[Fe(CRH_4)Cl_2]BF_4$ containing O_2 and acetate buffer. Only those results obtained using unbuffered catalyst stock solutions will be presented in the following sections.[41]

Table II. Dependence of Initial Rate on Initial Concentration of Catalyst $[Fe(CRH_4)Cl_2]BF_4$

$[[Fe(CRH_4)Cl_2]BF_4]_0$, M ($\times 10^4$)	rate, M s^{-1} ($\times 10^2$)	$[[Fe(CRH_4)Cl_2]BF_4]_0$, M ($\times 10^4$)	rate, M s^{-1} ($\times 10^2$)
0.72	0.653 ± 0.041	7.86	4.88 ± 2.24
1.24	0.728 ± 0.114	8.53	9.63 ± 1.01
1.73	1.43 ± 0.16	8.75	10.1 ± 0.71
3.24	2.82 ± 0.41	10.61	13.9 ± 0.71
4.05	5.46 ± 0.35	10.89	14.1 ± 3.27
5.09	5.82 ± 1.04	11.00	10.6 ± 1.48
6.16	4.47 ± 0.24	11.61	16.1 ± 1.6
6.47	6.99 ± 0.70	12.98	12.6 ± 1.95
6.58	6.75 ± 0.74	13.63	16.0 ± 0.78
7.45	8.47 ± 0.42	15.86	18.2 ± 1.41

Table III. Dependence of Rate on Initial Concentration of H_2O_2[a]

$[H_2O_2]_0$, M	$[H_2O_2]_0^2$, M^2	rate, M s^{-1} ($\times 10^2$)
0.0688	0.0047	1.27 ± 0.09
0.124	0.0154	5.08 ± 0.51
0.178	0.0317	8.22 ± 0.53
0.238	0.0569	15.5 ± 1.05
0.295	0.0872	21.0 ± 1.00
0.0985	0.0097	2.48 ± 0.12
0.11	0.0121	2.50 ± 0.13
0.1178	0.0139	3.70 ± 0.18
0.1237	0.0153	4.14 ± 0.21
0.136	0.0185	4.69 ± 0.24
0.182	0.033	7.82 ± 0.39
0.202	0.0408	9.83 ± 0.50
0.272	0.0740	13.3 ± 0.65
0.289	0.0835	20.9 ± 1.04
0.344	0.118	28.6 ± 1.42
0.36	0.1296	30.6 ± 1.50

[a] $[Fe]_0 = 6.58 \times 10^{-4}$ M, pH 4.61, $[OAc^-] = 0.051$ M.

The initial rate of hydrogen peroxide decomposition at constant $[H_2O_2]_0$ (0.182 M), pH (4.61), $[OAc^-]$ (0.0509 M), temperature (25 °C), and ionic strength ($\mu = 0.5$ M) was studied as a function of the initial concentration of $[Fe(CRH_4)Cl_2]BF_4$ in the concentration range between 0.7×10^{-4} and 15.9×10^{-4} M. Representative rate data are presented in Table II. Observed rates were converted to units of M/s by dividing observed rates in units of mol O_2/s by the volume of the reaction solution, 0.027 L (25 mL of peroxide solution + 2 mL of catalyst solution). A graph of initial rate vs. the initial concentration of $[Fe(CRH_4)Cl_2]BF_4$ yields a straight line conforming to the equation

$$\text{rate} = (1.178 \times 10^2)[[Fe(CRH_4)(H_2O)_2]^{+3}]_0 - 0.375 \times 10^{-2} \quad (4)$$

The intercept is zero within experimental error, implying that decomposition does not occur at an appreciable rate by a catalyst-independent path. The slope of the plot gives directly the value of k_{obsd}, which is a function of $[H_2O_2]_0$, pH, and $[OAc^-]$.

Dependence of Initial Rates on $[H_2O_2]_0$. Data representing the dependence of initial rate on $[H_2O_2]_0$ (the subscript "0" indicates initial concentration) show a second-order behavior (Table III). All rates were measured at an initial catalyst concentration of 6.58×10^{-4} M, pH 4.61, and $[OAc^-] = 0.0509$ M. The intercept of the plot is zero within experimental error, as expected. Since it has been established here that the rate depends on the square of the initial hydrogen peroxide

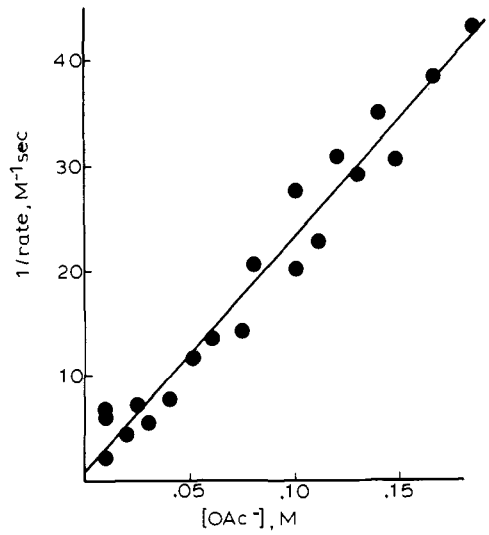

Figure 2. 1/rate vs. [OAc⁻]. Same concentration conditions as for Figure 1.

concentration, this dependence can be factored out of k_{obsd} calculated above. When this is done, the expression in eq 5 is obtained, where the third-order rate constant has units of M^{-2} s^{-1}.

$$\text{rate} = 3.5_6 \times 10^3[[Fe(CRH_4)(H_2O)_2]^{3+}]_0[H_2O_2]_0^2 \quad (5)$$

Dependence of Initial Rates on pH. The dependence of observed rate on pH suggested that a graph of rate vs. the reciprocal of hydrogen ion concentration be made. Such a plot confirms the expected linear behavior. The data in Table IV agree with the equation

$$\text{rate} = k_H \frac{[H_2O_2]_0^2[cat]}{[H^+]} \quad (6)$$

Dependence of the Initial Rate on the Concentration of Acetate Ion. Data for the dependence of initial rate on the concentration of acetate ion are presented in Table V. The hyperbolic appearance of a plot of rate vs. [OAc⁻] suggested that a more meaningful representation of the data might be achieved by plotting either 1/rate vs. [OAc⁻] or rate vs. 1/[OAc⁻]. The former plot is shown in Figure 2 and the latter in Figure 3.

$$\text{rate} = k_A \frac{[cat][H_2O_2]_0^2}{[H^+]} \frac{1}{1 + K_A[OAc^-]_0} \quad (7)$$

$$\text{rate} = k_B \frac{[cat][H_2O_2]_0^2}{[H^+][OAc^-]_0} \quad (8)$$

Both are seen to be linear, with near-zero intercepts. If significance is attributed to the intercept in Figure 2, a rate law of the form of eq 7 is implied. Least-squares analysis of the data in Figure 2 gives a slope of 222 and an intercept of 914. For the concentration of hydrogen ion (2.46×10^{-5} M), catalyst (6.58×10^{-4} M), and peroxide (0.182 M) used in the acetate dependence study, it follows that $k_A = 1.23$ M^{-1} s^{-1} and $K_A = 243$ M^{-1}. If, on the other hand, the intercept in Figure 3 is assumed zero within experimental error, a rate law of the form of eq 8 applies. The slope of the line in Figure 3 gives $k_B = 5.1 \times 10^{-3}$ s^{-1}. Both eq 7 and 8 imply by their forms a retardation of peroxide decomposition by acetate ion. As will be seen below, the former equation is not consistent with all our observations while the latter, which follows from a free-radical mechanism, is entirely consistent with all our data.

Dependence of the Rate on Temperature. The rate of peroxide decomposition was studied at temperatures in the range 8-32 °C at pH 4.61 and [OAc⁻] = 0.05 M. The observed

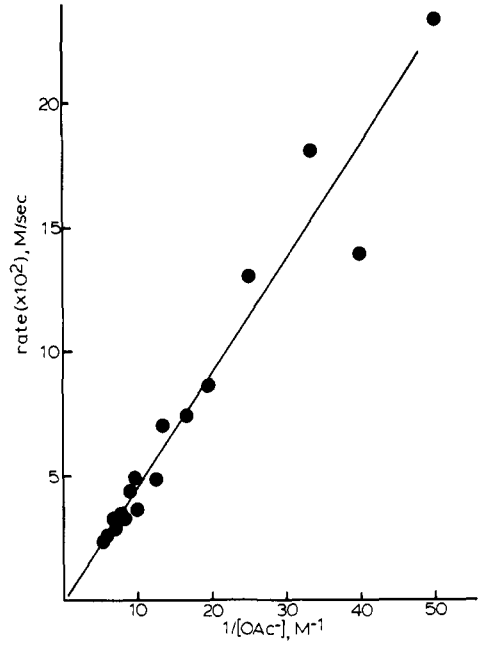

Figure 3. Rate vs. 1/[OAc⁻]

Table IV. Dependence of Initial Rate on Hydrogen Ion Concentration[a]

pH	$1/[H^+]$, M^{-1} ($\times 10^{-4}$)	rate, M s^{-1} ($\times 10^2$)
3.94	0.8724	2.42 ± 0.07
4.23	1.701	5.38 ± 0.27
4.61	4.082	8.61 ± 0.56
4.85	7.094	12.9 ± 1.61
5.11	12.91	15.6 ± 1.64
5.11	12.91	20.7 ± 1.80
4.40	2.51	8.29 ± 0.40
4.62	4.17	9.58 ± 0.48
4.80	6.31	14.2 ± 0.70
5.00	10.00	19.1 ± 0.90
5.10	12.59	24.6 ± 1.3

[a] $[Fe]_0 = 6.58 \times 10^{-4}$ M, $[H_2O_2]_0 = 0.182$ M, $[OAc^-] = 0.0509$ M.

Table V. Dependence of Initial Rate on Acetate Ion Concentration[a]

$[OAc^-]$, M	rate, M s^{-1} ($\times 10^2$)	$[OAc^-]$, M	rate, M s^{-1} ($\times 10^2$)
0.010	48.5	0.080	4.87
0.0102	16.6	0.100	3.63
0.0102	14.7	0.102	4.93
0.020	23.3	0.111	4.39
0.025	13.9	0.120	3.25
0.030	18.1	0.130	3.44
0.040	13.0	0.140	2.86
0.051	8.6	0.148	3.27
0.060	7.4	0.167	2.60
0.074	7.0	0.185	2.33

[a] $[Fe]_0 = 6.58 \times 10^{-4}$ M, $[H_2O_2]_0 = 0.182$ M, pH 4.61.

third-order rate constants, implicitly containing the concentrations of H^+ and OAc^-, were calculated and used to calculate the activation energy. The value of E_A, of 9 kcal mol^{-1}, is very similar to that obtained for Wang's TAEA complex but not comparable with that for catalase, which is 1 kcal mol^{-1}.

Discussion

There are at present two tenable models for the mechanism of decomposition of hydrogen peroxide by ferric-centered catalysts. The newest is that of Kremer,[10] who has proposed a mechanism formally analogous to that proposed for catalase and involving the formation of intermediate complexes containing iron in various oxidation states. The second mechanism involves free radicals, primarily the hydroxyl radical; it was first proposed by Haber and Weiss,[12,13] modified by Barb et al.,[14] and recently supported by Walling.[15] Our experimental results will now be discussed in terms of both mechanisms.

The "Intermediate Complex" Mechanism. As can be seen in Figure 2, our results appear to be consistent with a rate law of the form of (7), with $k_A = 1.23\ M^{-1}\ s^{-1}$ and $K_A = 243\ M^{-1}$. It remains to be seen whether retardation by acetate can be incorporated in a mechanism which is consistent with eq 7 in both qualitative and quantitative terms. The most obvious way to account qualitatively for such a rate law is to assume an equilibrium in which acetate interacts with the iron-containing catalyst to form a catalytically inactive complex. For instance, a stoichiometric mechanism like that in eq 9-13 might be invoked:

$$Fe(H_2O)(OH)^{2+} \underset{k_{-1}}{\overset{k_1}{\rightleftharpoons}} Fe(OH)^{2+} + H_2O \quad (9)$$

$$Fe(OH)^{2+} + OAc^- \underset{k_{-2}}{\overset{k_2}{\rightleftharpoons}} Fe(OH)(OAc)^+ \quad (10)$$

$$Fe(OH)^{2+} + H_2O_2 \underset{k_{-3}}{\overset{k_3}{\rightleftharpoons}} Fe(OH)(H_2O_2)^{2+} \quad (11)$$

$$Fe(OH)(H_2O_2)^{2+} \overset{K}{\rightleftharpoons} Fe(OH)(HO_2)^+ + H^+ \quad (12)$$

$$Fe(OH)(HO_2)^+ + H_2O_2 \overset{k_4}{\rightarrow} Fe(OH)_2{}^+ + H_2O + O_2 \quad (13)$$

The ligand designation, CRH_4, has been omitted from the formulas for brevity, and the pH dependence has been shown as involving deprotonation of bound rather than free peroxide, which is the most chemically reasonable formulation in the pH range involved. The rate law consistent with this mechanism, assuming (13) to be the rate-determining step and expressing the rate in terms of total iron concentration, is given in the equation

$$\frac{dO_2}{dt} = \frac{k_4 K K_1 K_3 [Fe][H_2O_2]^2}{[H^+](1 + K_1K_2[OAc^-] + K_1K_3[H_2O_2])} \quad (14)$$

which corresponds quite well with eq 7 if $k_A = k_4KK_1K_3$, $K_A = K_1K_2$, and $K_1K_3[H_2O_2]$ is negligible compared to the remaining terms in the denominator. The above mechanism is therefore qualitatively consistent with the experimentally observed rate law, provided that certain assumptions are made regarding the relative magnitudes of K_2 and K_3.

Quantitatively, however, the mechanism is untenable. The experimental rate law requires that the equilibrium constant for formation of the acetate complex (K_1K_2) have a value of $243\ M^{-1}$. At an acetate concentration of 0.05 M, this requires a value of about 12 for the ratio of the concentration of $[Fe(OH)(OAc)]^+$ to that of $[Fe(OH)(H_2O)]^{2+}$. However, such a high ratio is inconsistent with the results of our potentiometric titration studies which revealed no detectable interaction between $Fe(CRH_4)(OH)(H_2O)^{2+}$ and OAc^- under conditions similar to those of the kinetic studies. We are therefore forced to conclude that an equilibrium interaction between $[Fe(CRH_4)(H_2O)(OH)]^{2+}$ and OAc^- does not provide an acceptable explanation for the observed retardation by acetate. Instead it is conceivable that acetate retardation is explicable in terms of the mechanism proposed by Kremer[10-19] to explain catalysis of H_2O_2 decomposition by Fe^{3+} and hemin and catalase. The mechanism, which is a modification of the peroxidatic mechanism of Chance,[8] is as follows:

$$E + S \underset{k_{-1}}{\overset{k_1}{\rightleftharpoons}} C_I \quad (15)$$

$$C_I \underset{k_{-3}}{\overset{k_3}{\rightleftharpoons}} C_I' \quad (16)$$

$$C_I' + S \overset{k_4}{\rightarrow} E + P \quad (17)$$

$$C_I' + H_2A \overset{k_5}{\rightarrow} E + A + H_2O \quad (18)$$

Here, E = the iron-containing catalyst, S = hydrogen peroxide, C_I = a primary catalyst-substrate complex, C_I' = a secondary complex, formed by intramolecular alteration of C_I, P = the reaction products, namely, water and O_2, and H_2A = an oxidizable organic substrate (acetate). The pH dependence, which is relevant for all catalysts but catalase, has been omitted for simplicity. It is easily incorporated as shown by Kremer. Also, we have taken the liberty of including both the reverse of eq 16 and eq 18, which Kremer does not do. Assuming a steady state for C_I and C_I', expressing the rate law in terms of the total concentration of iron-containing species, and assuming (17) to be rate determining, the rate law in eq 19 is derived:

$$\frac{dP}{dt} = k_4[C_I'][S] = \left\{ \frac{k_1k_3k_4[E]_0[S]^2}{k_{-1}k_{-3} + k_1[S](k_3 + k_{-3}) + k_5[H_2A](k_{-1} + k_3) + k_1k_5[H_2A][S]} \right\} \quad (19)$$

Only by making a series of unfounded assumptions regarding the relative magnitudes of the terms in the denominator can eq 19 be cast in the form of eq 7. The essential aspect of this mechanism that causes it to contain the necessary inverse rate dependence on acetate is the addition of an irreversible process involving acetate. That is, this and other mechanisms that assume the irreversible reaction (oxidation) of acetate can, given enough assumptions, be made to fit the experimental rate law. For example, if eq 10 in the mechanism given by eq 9-13 is replaced by

$$Fe(OH)(H_2O_2)^{2+} + OAc^- \rightarrow Fe(OH)_2{}^+ + \text{oxidation of } OAc^- \quad (20)$$

then, again, a rate law of the generally appropriate form can be derived. While the lesson is the requirement that acetate enter into an irreversible process, the difficulty is that additional troublesome assumptions must be made. This difficulty does not arise in attempts to fit the rate law to the free-radical mechanism.

The Free-Radical Mechanism. For a general ferric-containing catalyst, abbreviated as (Fe^{3+}), the mechanism may be written as follows:

$$H_2O_2 + (Fe^{3+}) \overset{k_5}{\rightarrow} (Fe^{2+}) + H^+ + HO_2\cdot \quad (21)$$

$$(Fe^{2+}) + H_2O_2 \overset{k_6}{\rightarrow} (Fe^{3+}) + HO^- + HO\cdot \quad (22)$$

$$HO\cdot + H_2O_2 \overset{k_7}{\rightarrow} H_2O + HO_2\cdot \quad (23)$$

$$HO_2\cdot + (Fe^{3+}) \overset{k_8}{\rightarrow} O_2 + (Fe^{2+}) + H^+ \quad (24)$$

$$HO_2\cdot + (Fe^{2+}) \overset{k_9}{\rightarrow} HO_2^- + (Fe^{3+}) \quad (25)$$

Reaction 21 is the chain initiation step, (22-24) are propagating steps, and (25) is a termination step. Reactions 21 and 24 are both considered to be pH-dependent processes, involving prior acid dissolution equilibria. Retardation by organic materials is accounted for in this mechanism by assuming that they compete for chain-carrying OH· radicals via sequences such as

$$HO\cdot + RH \xrightarrow{k_{10}} H_2O + R\cdot \quad (26)$$

$$R\cdot + O_2 \xrightarrow{k_{11}} RO_2\cdot \quad (27)$$

$$RO_2\cdot + (Fe^{2+}) \xrightarrow{k_{12}} RO_2^- + (Fe^{3+}) \quad (28)$$

If chain termination is assumed to occur by this sequence instead of by eq 25, the following rate expressions can be derived by assuming steady-state concentrations for Fe^{2+}, OH ·, and HO_2·.[42]

$$\frac{-d[H_2O_2]}{dt} = 2k_5[Fe^{3+}][H_2O_2]\left(1 + \frac{k_7[H_2O_2]}{k_{10}[RH]}\right) \quad (29)$$

$$\frac{d[O_2]}{dt} = k_5[Fe^{3+}][H_2O_2]\frac{k_7[H_2O_2]}{k_{10}[RH]} \quad (30)$$

Equation 30 is of the same form as eq 8, the empirical rate law for the $Fe(CRH_4)(H_2O)(OH)^{2+}$-catalyzed decomposition (if the implicit pH dependence of k_5 is included). It is also significant that no additional assumptions need be made to bring the experimental and theoretical rate laws into correspondence. Unfortunately, we were not able to monitor the disappearance of hydrogen peroxide in our system and thus cannot experimentally verify the form of eq 29. We are therefore not able to obtain separate experimental determinations of k_5 and k_7/k_{10}, which would be necessary in order to compare our results with those from radiation chemistry. The linearity and zero intercept of the graph in Figure 3, however, are entirely consistent with the predictions of the free-radical mechanism, and do allow calculation of the quantity k_5k_7/k_{10}, giving the value 2.07×10^2 M^{-1} s^{-1}. This may be compared with the value 1.8×10^{-3}, obtained for the retardation of the Fe^{3+}-catalyzed decomposition by acetic acid at $[H^+] = 1.92 \times 10^{-2}$ M.[42] Correcting this value to pH 4.61 by assuming an inverse dependence on $[H^+]$ gives a value of 1.41 M^{-1} s^{-1} for k_5. Our value is therefore about two orders of magnitude larger than would be expected from results on aquo-ferric ion catalysis. Similar behavior has been observed for catalysis of peroxide decomposition by $Fe(EDTA)^-$, which gives slopes about ten times larger than expected.[43] The apparent explanation in the case of the EDTA system is that EDTA itself, both complexed and uncomplexed, is subject to attack by HO· radicals. Chain propagation is made more effective by this mechanism and retardation by acetic acid is thus less effective than in the absence of EDTA. The same type of mechanism is possible in our system. The CRH_4 ligand is largely saturated and thus susceptible to hydrogen abstraction by OH·. The resulting radical would be very rapidly oxidized via a cage reaction by the Fe^{3+} to which it is coordinated, thus regenerating Fe^{2+} for chain propagation. Such cage reactions might be expected to be very favorable for a macrocyclic ring which is effectively locked into position about the iron atom. An additional enhancement of a power of about 10 seems reasonable in this context. Further evidence that a mechanism of this type may be operative is the relatively short lifetime of the $Fe(CRH_4)(H_2O)(OH)^{2+}$ catalyst. The number of molecules of H_2O_2 decomposed per molecule of $Fe(CRH_4)(H_2O)(OH)^{2+}$ initially present is quite small, indicating that the macrocyclic ligand is altered during the decomposition. Finally, we have observed that ethanol retards peroxide decomposition; this provides further support for the possibility of a free-radical mechanism.

Table VI. Catalytic Activity of Ferric-Centered Complexes[a]

catalyst	activity, M^{-1} s^{-1} [b]	E_{A_1}, kcal/mol
catalase	10^6–10^7	1
hemin	10^3–10^4 [c]	
$Fe(trien)^{3+}$	10^2	6.6
Fe^{3+}(aqueous)	10^4 [c]	20
$Fe(CRH_4)^{3+}$	10^5	9

[a] Reference 16. [b] All values appropriate to 25 °C, pH 7, expect those for Fe^{3+} and hemin, which apply to 0 °C. [c] Reference 18.

Relative Catalytic Abilities of Model Complexes. In Table VI are presented the catalytic activities, defined as second-order observed rate constants, for most of the known Fe(III)-centered catalysts for peroxide decomposition. In order to put our rate law in the appropriate form, we must include the first power of the peroxide concentration as a factor in the rate constant. When k_{obsd} from eq 5, 3.56×10^3 M^{-2} s^{-1}, is multiplied by 0.182 M, a median value for the concentration of peroxide, the peroxide-dependent second-order rate constant shown in the table is obtained. If rate constants measured at or extrapolated to pH 7 are compared, it is seen that $[Fe(CRH_4)Cl_2)Cl_2]BF_4$ ranks very high, keeping in mind, of course, the peroxide-dependent nature of the activity.

Acknowledgment. These studies were supported by Grant GM 10040 from the National Institute of General Medical Sciences of the U.S. Public Health Service.

References and Notes

(1) See S. Hoeffling, *J. Prakt. Chem.*, **89**, 334 (1964).
(2) N. Stoecklin, *C. R. Acad. Sci.*, **152**, 729 (1911).
(3) P. Nicholls and G. R. Schonbaum in "The Enzymes", Vol. 8, P. D. Boyer, H. Lardy, and K. Myrback, Eds., Academic Press, New York, 1963, pp 147–225.
(4) B. Chance, *Arch. Biochem.*, **21**, 416 (1949).
(5) P. George in "Currents in Biochemical Research", D. E. Green, Ed., Wiley-Interscience, New York, 1956, p 338.
(6) D. Dolphin and R. H. Felton, *Acc. Chem. Res.*, **7**, 26 (1974).
(7) P. Jones and A. Suggett, *Biochem. J.*, **110**, 621 (1968).
(8) B. Chance, D. S. Greenstein, and F. J. W. Roughton, *Arch. Biochem. Biophys.*, **37**, 301 (1952).
(9) B. Chance, *Tech. Org. Chem.*, **8**, *1314 (1963)*.
(10) M. L. Kremer, *Isr. J. Chem.*, **9**, 321 (1971).
(11) E. Zidoni and M. L. Kremer, *Arch. Biochem. Biophys.*, **161**, 658 (1974).
(12) F. Haber and J. Weiss, *Naturwissenschaften*, **20**, 948 (1932).
(13) F. Haber and J. Weiss, *Proc. R. Soc. London, Ser. A*, **147**, 332 (1934).
(14) W. C. Barb, J. H. Baxendale, P. George, and K. R. Hargrave, *Trans. Faraday Soc.*, **47**, 462, 591, 935 (1951).
(15) C. Walling, *Acc. Chem. Res.*, **8**, 125 (1975).
(16) S. B. Brown, P. Jones, and A. Suggett, *Prog. Inorg. Chem.*, **13**, 159 (1970).
(17) M. M. Taqui Khan and A. E. Martell, "Homogeneous Catalysis by Metal Complexes", Vol. I, Academic Press, New York, 1974.
(18) S. B. Brown, T. C. Dean, and P. Jones, *Biochem. J.*, **117**, 741 (1970).
(19) M. L. Kremer, *Biochim. Biophys. Acta*, **297**, 268 (1973).
(20) P. Jones, T. Robson, and S. B. Brown, *Biochem. J.*, **135**, 353 (1973).
(21) A. H. Cook, *J. Chem. Soc.*, 1761 (1938).
(22) J. H. Wang, *J. Am. Chem. Soc.*, **77**, 882 (1955).
(23) J. H. Wang, *J. Am. Chem. Soc.*, **77**, 4715 (1955).
(24) R. C. Jarnagin and J. H. Wang, *J. Am. Chem. Soc.*, **80**, 786 (1958).
(25) R. C. Jarnagin and J. H. Wang, *J. Am. Chem. Soc.*, **80**, 6477 (1958).
(26) M. T. Beck and S. Gorog, *Acta Chim. Acad. Sci. Hung.*, **20**, 57 (1959).
(27) M. T. Beck and S. Gorog, *Acta Phys. Chem.*, 70 (1958) (Symposium on Complex Chemistry).
(28) C. Walling, M. Kurz, and H. J. Schugar, *Inorg. Chem.*, **9**, 931 (1970).
(29) P. Merrell, Ph.D. Thesis, The Ohio State University, 1971.
(30) J. L. Karn and D. H. Busch, *Inorg. Chem.*, **8**, 1149 (1969).
(31) J. D. Curry and D. H. Busch, *J. Am. Chem. Soc.*, **86**, 592 (1964).
(32) D. F. Evans, *J. Chem. Soc.*, 2003 (1959).
(33) D. P. Riley, P. H. Merrell, J. A. Stone, and D. H. Busch, *Inorg. Chem.*, **14**, 490 (1975).
(34) I. G. Sayce, *Talanta*, **15**, 1397 (1968).
(35) The conversion is made by multiplying the observed recorder deflection, in units of cm along the pressure axis divided by cm along the time axis, by the following factors: (1) chart speed (cm/s), usually either 2.5 or 5 cm/s; (2) number of precision pressure gage units (~23 000 units are equivalent to 1 atm) per cm of recorder deflection; (3) pressure change (atm) per precision pressure gage unit; (4) moles O_2 produced per unit pressure change, in atm ($\Delta n/\Delta p = V/RT$, where V = the volume of the vacuum system + reaction flask (see below) and T = the absolute temperature). The pressure change (atm) per precision pressure gage unit was calculated from the factory calibration data supplied with the instrument, and has the

value 4.176 96 × 10^{-5} atm/unit. The number of precision pressure gage units per cm of recorder deflection depends upon the recorder range selected.
(36) W. Garbett, D. W. Darnall, I. M. Klotz, and R. J. P. Williams, *Arch. Biochem. Biophys.*, **135**, 419 (1969).
(37) V. L. Goedken and D. H. Busch, *J. Am. Chem. Soc.*, **94**, 7355 (1972).
(38) M. C. Rakowski, M. Rycheck, and D. H. Busch, *Inorg. Chem.*, **14**, 1194 (1975).
(39) H. J. Schugar, G. R. Rossman, C. G. Barraclough, and H. B. Gray, *J. Am. Chem. Soc.*, **94**, 2683 (1972).
(40) K. S. Murray, *Coord. Chem. Rev.*, **12**, 1 (1974).
(41) The details of the correction for dimer formation are too lengthy to present here, but may be obtained on request.
(42) C. Walling and A. Goosin, *J. Am. Chem. Soc.*, **95**, 2987 (1973).
(43) C. Walling, R. C. Partch, and T. Weil, *Proc. Natl. Acad. Sci. U.S.A.*, **72**, 140 (1975).

Ring Size Limits for the Direct Observation of Hydrido-Bridged Secondary Cycloalkyl Cations. Correspondence with Chemical Reactivity Studies

Roger P. Kirchen and Ted S. Sorensen*

Contribution from the Department of Chemistry, University of Calgary, Calgary, Alberta T2N 1N4, Canada. *Received November 27, 1978*

Abstract: The direct observation of stable hydrido-bridged cycloalkyl cations, in rings containing 8–11 carbon atoms, corresponds exactly with those cycloalkyl rings where direct transannular hydrogen shifts have been observed in reactions involving a presumed carbocation intermediate. Within this observable ion series, there are interesting variations in both the ion reactivity and in the NMR properties. For rings of 8, 9, and 11 carbons, the corresponding 1-methyl 7-, 8-, and 10-carbon tertiary ion is formed, whereas the 10-membered hydrido-bridged ion eliminates hydrogen and forms the decalyl cation. The NMR results show that decreases in the chemical shift of the two terminal hydrogens are matched by a corresponding increase in the chemical shifts of the bridging hydrogen. This behavior is consistent with theoretical models which crudely picture the bonding as a hydride ion centered between two cationic centers. The *negative* charge on the bridging hydrogen increases as the separation of the two bridged carbons is increased. Correspondingly, the terminal protons experience an increased *positive* charge.

The classic studies by Prelog and Cope and their respective co-workers[1] beginning in 1952 have established that cycloalkyl rings from C_8 to C_{11} undergo direct transannular hydride shifts in reactions involving a carbocation intermediate. This reactivity was not observed for C_{12} systems and only in a minor way for the C_7 case. We have recently prepared the observable C_{10} cyclodecyl cation[2,3] and have suggested, based on the very unusual ^1H NMR spectrum, that this ion possesses a μ-hydrido-bridged structure **1**.

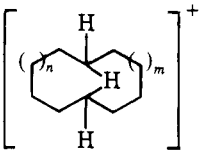

1, $n = m = 1$ and $n = 2$, $m = 0$[4]

Since the cyclodecyl cation transannular chemistry is not unique to this ring size, one may wonder whether hydrido bridging might also be observed in other rings.[5] The purpose of this paper is to show that, indeed, this is the case. With the complete bridged-ion series from $n = 8$ to $n = 11$ now available, one notes very interesting comparative differences in both structure and reactivity.

Results

The most difficult cation to "observe" is the cyclooctyl member. Cyclooctyl chloride in $CFCl_3$ was added to a mixture of SbF_5 in SO_2ClF-SO_2F_2 at ca. −143 °C[6] (or *cis*-cyclooctene using 1:1 SbF_5-FSO_3H, same solvent), and the NMR spectrum of the resulting solution was obtained as quickly as possible (−147 °C, up to as high as −141 °C in one case). These spectra always indicated a mixture of two carbocations,[7] one being the known 1-methylcycloheptyl cation **2**.[8] The second species is characterized chemically by its very rapid conversion into **2**, $t_{1/2}$ = ca. 17 min at −142 °C, $\Delta G^{\ddagger}$ = ca. 9.3 kcal/mol. The ^{13}C NMR spectrum consists of four lines, δ 151.7 (2 C), 50.6 (1 C), 41.3 (1 C), and 31.5 (4 C). However, the most distinctive spectral features are the characteristic very high field ^1H signal at δ −7.7 and low field signal at δ 7.9, these having an area ratio of 1:2[9] (see Figure 1). These protons are coupled to the low field carbon peak at δ 151.7 with J = <35[10] and 147 ± 10 Hz, respectively. This situation is very reminiscent of that found in the cyclodecyl cation **1** and allows one to assign this ion as **3**. The ^{13}C NMR results[11] indicate that the

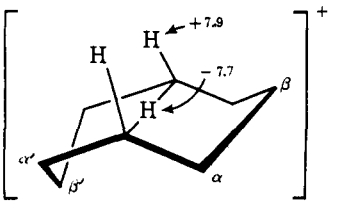

3

β carbons are nonequivalent and this fits with the chair-boat formulation shown in **3**, a conformation similar to that previously proposed for the 1-methylcyclooctyl cation.[8] We have not attempted quenching experiments on this ion (or the C_9 and C_{11} analogues) because of the extreme instability; how-

0002-7863/79/1501-3240$01.00/0